applied sciences

MDPI

Article

Development of the Galerkin Finite Element Method for Stress-Based Elasticity Problems

Abduvali A. Khaldjigitov [1], Akmal A. Bobonazarov [1], Umidjon Z. Djumayozov [2,*], Otajon U. Tilovov [1,3], Suratjon P. Pulatov [2], Maftuna N. Abdirakhmonova [4] and Fazilat S. Ochilova [2]

1 Department of Mechanics and Mathematical Modeling, Faculty of Mathematics, National University of Uzbekistan, Street Universitetskaya 4, Tashkent 100174, Uzbekistan
2 Department of Software Engineering, Faculty of Artificial Intelligence and Digital Technologies, Samarkand State University, University Boulevard 15, Samarkand 140104, Uzbekistan
3 Department of Econometrics, Tashkent State University of Economics, Karimov Street 49, Tashkent 100066, Uzbekistan
4 Department of Computer Engineering, Faculty of Computer Engineering, Samarkand State University, University Boulevard 15, Samarkand 140104, Uzbekistan
* Correspondence: djumayozov@bk.ru

Abstract

This paper proposes a finite element approach to the numerical solution of boundary value problems of linear elasticity theory formulated directly in terms of the stress tensor components. In contrast to the classical finite element formulation, in which displacements are the primary unknowns, the approach considered here treats the stress components as the sought quantities. Two forms of the boundary value problem are investigated. The first is based on the joint use of the equilibrium equations and the Beltrami–Michell equations, while the second is a transformed system of Poisson-type equations for the stress tensor components. Variational relations based on the Galerkin method are obtained for both formulations. Using linear basis functions on triangular finite elements, local matrices are constructed, and global systems of algebraic equations are formed, whose unknowns are the nodal values of the stresses. The numerical implementation of the developed schemes is carried out in an in-house C++ program and in the FreeFEM++ software environment. To verify the reliability of the proposed mathematical and numerical models, the classical Kirsch problem of a stretched elastic plate with a circular hole—characterized by a pronounced stress concentration near the edge of the hole—is solved. The numerical values of the stress components are compared with the analytical solution obtained using the Airy stress function method, as well as with the results of calculations performed with the FreeFEM++ software package. The comparison shows good agreement between the obtained solutions and confirms the possibility of determining stresses directly, without first computing the displacement field. A mesh-refinement study further showed a systematic reduction in the numerical error: on the finest mesh considered, the relative error decreased to 3.189% for formulation A and to 7.415% for formulation B. The proposed approach extends the applicability of the finite element method to boundary value problems of elasticity theory formulated in terms of stresses and can be used to study problems with complex geometry and local stress concentration.

Keywords: stress-based formulation; linear elasticity; Beltrami–Michell equations; Poisson equations for stresses; Galerkin method; finite element method; stress tensor; Kirsch problem; stress concentration

Received: 26 August 2026
Revised: 14 September 2026
Accepted: 17 September 2026
Published: 19 September 2026

1. Introduction

Elasticity theory is one of the fundamental branches of the mechanics of deformable solids and serves as the mathematical basis for studying the stress–strain state of structural elements and continuous media. Within the framework of linear elasticity theory, the state of a body is determined by the interrelated fields of displacements, strains, and stresses, which satisfy the equilibrium equations, the geometric and physical relations, and the corresponding boundary conditions. In the classical formulation, boundary value problems are predominantly formulated in terms of the displacement vector components. Once the displacements have been determined, the strain components are computed by differentiating them, and the stresses are then recovered using the constitutive relations of elasticity theory. This approach is widely used in analytical and numerical methods and forms the basis of most conventional finite element schemes.

At the same time, in many applied problems the primary interest lies directly in the stress distribution, particularly in regions of local stress concentration near holes, notches, boundaries, and other geometric discontinuities. When a displacement-based formulation is used, stresses are secondary quantities, and their computation involves differentiating the approximate displacement field. In numerical calculations, this can affect the accuracy of determining the local characteristics of the stress state and requires additional post-processing of the obtained solution. This makes it of interest to develop alternative mathematical and numerical formulations in which the stress tensor components serve directly as the primary unknown functions.

Formulating boundary value problems directly in terms of stresses requires the simultaneous satisfaction of the equilibrium equations and the compatibility conditions, which, after eliminating the strains, lead to the Beltrami–Michell equations. Such a formulation makes it possible to treat the stress state as an independent object of mathematical modeling; however, constructing a closed system of equations, correctly specifying the boundary conditions, and developing an efficient numerical scheme remain more complex than in the traditional displacement-based formulation. Therefore, the development of direct methods for solving boundary value problems in terms of the stress tensor components, including those based on variational principles and the finite element method, represents an independent and relevant direction of computational mechanics.

Ref. [1] systematizes the fundamental principles of classical elasticity theory, including the equilibrium equations, the physical and geometric relations, the strain compatibility conditions, and methods for solving two-dimensional boundary value problems. Particular attention is given to the analytical determination of the stress state of elastic bodies, including problems characterized by local stress concentration. The presented results form the theoretical basis for the further development of mathematical and numerical methods for solving boundary value problems of elasticity theory.

Further development of the classical concepts of elasticity theory is presented in [2], which considers the basic equations of spatial and plane problems, various ways of describing the stress–strain state, and the corresponding boundary conditions. Formulations relating stresses to the equilibrium equations and compatibility conditions are of particular significance. From a mathematical standpoint, these principles were further developed in [3], which systematizes various forms of the equations of elasticity theory and the relations between displacements, strains, and stresses. The approaches considered create a theoretical basis for the transition from the traditional displacement-based formulation to formulations in which the stress tensor components can be treated as independent unknown functions.

In modern research, the classical principles of elasticity theory have been further developed toward a more detailed analysis of the stress–strain state and the construction of efficient numerical methods. Ref. [4] systematizes theoretical and computational

https://doi.org/10.3390/app16189303

approaches to solving elasticity problems, including methods for determining the displacement, strain, and stress fields in bodies of complex geometry. Ref. [5] considers mathematical formulations of elasticity and thermoelasticity problems based on the interrelation of mechanical and physical relations, and presents approaches to formulating the corresponding boundary value problems. The transition from a continuous mathematical model to its finite element approximation is described in detail in [6], which formulates the basic principles of the variational representation, the discretization of the computational domain, and the construction of systems of algebraic equations. These results formed the fundamental basis of the finite element method and created the prerequisites for developing its various modifications, including formulations in which, along with or instead of displacements, the stress components are treated as the primary unknowns.

The finite element method has been further developed through improvements in variational formulations and in the ways of approximating the primary sought quantities within a finite element. Ref. [7] systematizes issues in constructing finite element models for a broad class of engineering problems, including the choice of approximating functions, the formation of elemental and global systems of equations, and the implementation of boundary conditions. The mathematical foundations of the variational approach are presented in [8], which considers the transition from the differential formulation of a boundary value problem to the weak form underlying the Galerkin method and the subsequent finite element discretization. A fundamentally different aspect of elasticity theory is examined in [9]: the properties of a boundary value problem formulated directly in terms of the stress tensor components are considered, and the conditions necessary for constructing a consistent stress-based formulation are analyzed. Ref. [10] investigates the conservation laws of linear elasticity theory in a stress-based representation and shows their connection with the structure of the constitutive equations. These results are of substantial significance for direct stress-based formulations, since they confirm the possibility of treating the stress field as an independent object of the boundary value problem and form the theoretical prerequisites for constructing the corresponding variational and numerical methods.

The questions of completeness and closure of stress-based formulations have been further developed in [11], which proposes a complete Beltrami–Michell formulation for the analysis of axisymmetric elastic bodies and considers the role of additional relations in constructing a boundary value problem directly in terms of stresses. Ref. [12] investigates generalized solutions of weakened equations of elasticity theory with respect to the stress tensor components, which made it possible to refine the mathematical structure of the corresponding differential relations and the conditions for their satisfaction. The analysis of compatibility conditions is of particular significance for forming closed stress-based formulations. Ref. [13] considers the number of independent strain compatibility equations and the corresponding boundary conditions required for a consistent description of the strain field. Taken together, these results show that the transition to a direct stress-based formulation requires not only satisfying the equilibrium equations but also correctly accounting for the compatibility conditions and the structure of the Beltrami–Michell equations, which directly affects the mathematical closure of the boundary value problem and the subsequent construction of its numerical approximation.

The transition from theoretical stress-based formulations to their finite element implementation is presented in a number of studies. Ref. [14] proposes a stress-based finite element formulation for dynamic elastoplastic analysis, demonstrating the possibility of directly using stresses as the primary field variables in the discretization of mechanics problems. Ref. [15] develops a locally conservative stress-recovery procedure for the continuous Galerkin method in linear elasticity theory, aimed at improving the quality of the computed stress field and ensuring the local satisfaction of the equilibrium conditions.

Further development of the equilibrium approach is presented in [16], which constructs a higher-order finite element method with approximation of stress fields satisfying local equilibrium conditions and investigates its convergence properties. Ref. [17] extends stress-based finite element formulations to nonlinear analysis, where the stress components are treated as the primary unknown variables rather than quantities recovered from a previously computed displacement field. The formulation demonstrates that a direct approximation in terms of stresses can also be constructed beyond the framework of linear elasticity. In this approach, the nonlinear constitutive behavior is incorporated directly into the stress-based numerical formulation, thereby extending the range of problems for which stress variables can serve as the principal unknowns. For two-dimensional linear elasticity, the study in [18] develops a finite element methodology formulated directly in terms of stresses. The approach is based on the construction of admissible equilibrium stress fields and an associated variational formulation. Consequently, equilibrium requirements play a central role in defining the approximation space and in constructing the corresponding finite element equations. This provides an important alternative to the conventional displacement-based finite element formulation and demonstrates the feasibility of obtaining the stress field directly within a finite element framework.

Taken together, studies [14–18] demonstrate the progressive development of stress-based finite element methods, ranging from specialized stress approximations to more general variational formulations. However, these approaches are generally based on specifically constructed equilibrium stress fields, specialized variational principles, or additional requirements imposed on the approximation spaces. In contrast, the present study considers a direct Galerkin discretization of second-order differential equations written explicitly in terms of the stress tensor components. The stress components are used directly as the primary nodal unknowns and are approximated by standard continuous linear shape functions on triangular finite elements. No preliminary displacement solution is introduced for subsequent stress recovery. This distinction provides the basis for the two stress-based formulations considered below and for their implementation within a unified finite element framework.

Further development of finite element methods is associated with the use of mixed formulations, in which stresses are introduced as independent field variables alongside displacements or other characteristics of the stress–strain state. A multipoint stress mixed finite element formulation for linear elasticity on simplicial meshes is developed in [19]. In this approach, the stress tensor is treated as a primary independent variable together with the displacement field, while the finite element spaces are constructed to preserve the equilibrium structure of the elasticity problem. The multipoint approximation provides an efficient treatment of the discrete system and allows the stress field to be determined directly while maintaining local equilibrium. Thus, the method avoids recovering stresses solely by differentiating an approximate displacement field; however, it remains a mixed formulation in which both stress and displacement variables are involved. Ref. [20] presents a stress-based finite element formulation for two- and three-dimensional problems, based on the direct approximation of the stress components and aimed at improving the accuracy of their determination. For dynamic problems, [21] proposes a hybrid equilibrium finite element with higher-order stress fields, making it possible to improve the description of the stress state in elastic dynamic analysis. The possibilities of a direct stress-based formulation applied to one-dimensional structures are investigated in [22], where a stress-based FEM is used to compute the bending of Euler–Bernoulli and Timoshenko beams on an elastic foundation. Another class of mixed formulations is developed in [23], which constructs a compatible-strain mixed finite element method for two-dimensional compressible nonlinear elasticity, based on the independent representation of the strain variables and the satisfaction of their compatibility conditions. Ref. [24]

https://doi.org/10.3390/app16189303

extends this approach to incompressible nonlinear elasticity, accounting for the constraints arising from the incompressibility condition. In turn, [25] investigates symmetric mixed finite element formulations for elastodynamics problems and analyzes the corresponding space–time discretization. The approaches considered show that the direct inclusion of stresses or strains among the independent unknowns extends the possibilities of finite element modeling, but requires reconciling the function spaces, the compatibility conditions, and the stability of the mixed discretization.

The scope of application of stress-based and mixed finite element formulations is gradually extending from classical linear elasticity to more complex mechanical models. Thus, the possibility of using stress-based FEM to describe dynamic processes is shown in [26], while in [27] the assumed-stress formulation is extended to hyperelastic materials, accounting for the nonlinearity of the constitutive relations. Another approach is based on the independent approximation of strains: in [28], a compatible-strain mixed formulation is constructed for three-dimensional compressible and incompressible problems of nonlinear elasticity. For problems with a more complex structure of differential operators, [29] proposes a mixed discontinuous Galerkin scheme for linear viscoelasticity with a symmetric stress tensor, while [30] uses a similar discretization concept in stress space to solve the spectral problem of linear elasticity. Along with finite element schemes, variational methods are being developed that make it possible to directly include stresses in the discrete formulation. In particular, [31] uses the Hu-Washizu principle to construct a self-stabilized virtual element formulation for two-dimensional linear elasticity. Among the existing stress-based approaches, the formulations developed in [32,33] are particularly relevant to the present study. In [32], a finite element approximation for linear elasticity is constructed with the stress tensor as the principal field variable, providing a framework in which stresses are determined directly rather than recovered from a previously computed displacement solution. The formulation is developed from the governing relations of elasticity expressed in terms of stresses and is accompanied by an appropriate variational setting for the finite element approximation. A more comprehensive mathematical formulation is presented in [33], where two- and three-dimensional linear elasticity problems are expressed exclusively in terms of the components of the stress tensor. The governing stress equations, associated boundary conditions, and corresponding variational formulations are systematically derived, providing a consistent stress-only description of the elasticity problem. Particular attention is given to the mathematical structure of the stress formulation and to the construction of function spaces suitable for its variational treatment and finite element approximation. These results demonstrate that linear elasticity can be formulated and discretized without introducing the displacement field as a primary unknown and provide an important theoretical basis for the further development of stress-based finite element methods.

At the same time, an alternative direction retains the joint use of several field variables; for example, [34] proposes a stress-hybrid virtual element method for compressible and nearly incompressible materials on quadrilateral meshes. Thus, modern studies demonstrate a steady transition from recovering stresses from a computed displacement field to their direct inclusion in the variational and discrete formulation of the problem. However, the mathematical constructions used for this purpose differ substantially—ranging from mixed and discontinuous Galerkin formulations to hybrid and pure-stress approaches—leaving open the question of constructing a sufficiently simple, direct Galerkin scheme for a boundary value problem formulated directly in terms of the stress tensor components.

The current stage in the development of computational mechanics methods is characterized by efforts to improve the accuracy of stress determination by including stresses directly in the system of independent variables. One such approach is implemented in

[35] on the basis of a stress-hybrid virtual element method for six-node triangular elements; the proposed scheme is oriented toward solving problems for both compressible and nearly incompressible materials. A somewhat different principle is used in [36], which, for thin-walled structures, justifies the need for independent interpolation of stresses within a stabilized stress-displacement scheme. The possibilities of this methodology under large deformations are investigated in [37] for the case of finite hyperelasticity. A more complex structure of independent variables is adopted in [38]: for incompressible finite elasticity, a four-field mixed model is formulated, in which stresses enter the system alongside other field quantities.

For evaluating methods oriented toward the direct computation of stresses, problems with a known analytical solution and a pronounced stress gradient are of particular value. Among these is the classical Kirsch problem [39], which describes the stress field in an elastic plate with a circular hole under external loading. Its solution makes it possible not only to verify the distribution of individual stress tensor components but also to assess the ability of a numerical method to reproduce the stress concentration near the edge of the hole. In [40], the Kirsch problem is investigated from the standpoint of a boundary value formulation, which is of additional interest when analyzing ways of specifying and determining stresses on the boundary of the computational domain. The availability of an analytically determined stress field makes this problem a convenient benchmark for the quantitative verification of a finite element method constructed directly for the unknowns σ_{11}, σ_{22} and σ_{12}.

The issues of stress concentration and the possibility of reducing it for regions with holes are investigated in [41], which considers the application of a functionally graded layer in the vicinity of a pair of circular holes. A similar approach is used in [42] to assess the influence of various functionally graded materials on the magnitude of stress concentration near a hole. Ref. [43] proposes a stress-based formulation for modeling fiber-reinforced plates with cutouts, demonstrating the applicability of direct stress analysis to structures with geometric stress concentrators. A numerical implementation of boundary value problems directly in terms of stresses is presented in [44] using a finite-difference approach. Ref. [45] investigates the equilibrium of a three-dimensional elastic body with the stress tensor components chosen as the sought functions. The possibilities of a software implementation of the finite element method, including the construction of variational forms and the discretization of boundary value problems, are considered in [46]. The practical aspects of applying variational methods to mathematical problems of mechanics are presented in [47] and serve as the basis for the transition from a differential formulation to the corresponding weak form.

In contrast to mixed, hybrid, and stress-hybrid finite element formulations, in which additional unknowns, specialized function spaces, or stabilization conditions may be introduced together with the stresses, the present work considers a direct Galerkin scheme for a boundary value problem formulated in terms of the stress tensor components. The nodal stress values are used as the primary unknowns, and the discretization is performed using standard continuous linear basis functions on triangular finite elements. This approach makes it possible to investigate both formulations considered within a unified computational framework and to directly compare their numerical behavior under identical discretization conditions.

Despite the considerable development of finite element methods for elasticity problems, most existing approaches are still based on the displacement-based formulation or on mixed and hybrid formulations, in which stresses are introduced together with other field variables. Direct formulations of boundary value problems in terms of the stress tensor components have been investigated to a considerably lesser extent. In particular, finite element schemes that are constructed directly on the basis of the Beltrami–Michell equations and do not require the prior determination of the displacement field remain insufficiently developed.

Existing stress-based methods use various mixed, hybrid, discontinuous Galerkin, and virtual element formulations, which provide the required discretization properties but generally lead to the introduction of additional unknowns, special function spaces, or stabilizing conditions. At the same time, it remains relevant to construct a more direct scheme, in which the original boundary value problem is formulated solely in terms of the stress tensor components, and its numerical implementation is carried out within the framework of the standard Galerkin variational approach.

Of particular interest is the transformation of the Beltrami–Michell equations into a system of Poisson-type equations for the individual stress tensor components and the construction, on this basis, of the corresponding finite element discretization. A comparative analysis of the original Beltrami–Michell formulation and the transformed Poisson-type formulation within a single Galerkin method, including verification of the obtained solutions on a problem with a known analytical stress distribution, remains insufficiently represented in the existing literature. This is precisely the question that constitutes the main subject of the present study.

The aim of the present work is to develop a Galerkin finite element method for solving boundary value problems of linear elasticity theory formulated directly in terms of the stress tensor components. The system comprising the equilibrium equations and the Beltrami–Michell equations is considered as the original mathematical model. Along with this formulation, a transformed form of the problem is investigated, in which the Beltrami–Michell equations are reduced to Poisson-type equations for the stress tensor components.

For both formulations, the corresponding variational relations are constructed using the Galerkin method, and their finite element discretization is carried out using linear basis functions on triangular elements. Local finite element matrices are obtained, and global systems of algebraic equations are formed, whose unknowns are directly the nodal values of the stress tensor components. The numerical implementation of the developed method is carried out in a C++ program, and an independent verification of the results is performed using FreeFEM++ v4.12. The performance of the proposed schemes is investigated on the classical Kirsch problem for an elastic plate with a circular hole. The obtained stress distributions are compared with the analytical solution based on the Airy stress function and with the results of an independent finite element calculation. This comparison makes it possible to assess the correctness of the constructed variational formulations and the accuracy of the direct computation of the stress tensor components.

The scientific novelty of the work lies in the development of a finite element approach to solving boundary value problems of linear elasticity theory directly in terms of the stress tensor components. In contrast to the traditional displacement-based formulation, the stress components are treated as the primary unknowns and are determined directly from the corresponding system of differential equations. For the Beltrami–Michell equations, a Galerkin variational formulation is constructed, and its finite element approximation on triangular elements is obtained. Along with the original system, it is proposed to use a transformed formulation based on Poisson-type equations for the stress tensor components, for which an independent Galerkin scheme is also constructed. Local finite element matrices and an algorithm for forming the global system of algebraic equations directly in terms of the nodal stress values are obtained. Thus, both formulations are considered within a unified finite element approach, which makes it possible to compare their numerical solutions without first determining the displacement field. The correctness of the developed schemes is confirmed on the Kirsch problem by comparison with the analytical solution and an independent calculation in FreeFEM++. The obtained results

https://doi.org/10.3390/app16189303

demonstrate the possibility of directly determining the stress field by the finite element method, including in regions of local stress concentration.

The main novelty of the present work lies in the construction of a direct Galerkin finite element scheme in which the components of the stress tensor are treated as the primary nodal unknowns. In contrast to mixed and hybrid variational formulations, the proposed approach does not require the preliminary computation of the displacement field. For both formulations considered, weak forms and the corresponding finite element equations are derived using standard continuous linear basis functions on triangular elements, which enables their numerical comparison under identical discretization conditions.

2. Stress-Based Formulation of Plane Elasticity Problems

Let us consider a linearly elastic isotropic body occupying a domain Ω with boundary $B.$ In contrast to the classical displacement-based formulation, in what follows the stress tensor components are taken as the primary unknown functions. This formulation requires the simultaneous satisfaction of the equilibrium equations and the strain compatibility conditions expressed in terms of stresses, i.e., the Beltrami–Michell equations, together with the corresponding boundary conditions. Below, the original three-dimensional formulation is successively reduced to a plane problem, which is then used to construct the variational formulation and the finite element approximation by the Galerkin method.

It is known that a boundary-value problem of elasticity theory formulated in terms of stresses consists of three equilibrium equations

$$\sigma_{ij,j} + X_i = 0, \tag{1}$$

six Beltrami–Michell equations

$$\nabla^2\sigma_{ij} + \frac{1}{1+\nu}S_{,ij} = -(X_{i,j} + X_{j,i}) - \frac{\nu}{1-\nu}\delta_{ij}X_{k,k}, \quad S = \sigma_{kk}, \tag{2}$$

with the corresponding boundary conditions

$$\sigma_{ij}n_j\big|_{\Sigma_2} = S_i, \tag{3}$$

$$(\sigma_{ij,j} + X_i)\big|_{\Sigma} = 0. \tag{4}$$

where $\sigma_{ij} -$ is the stress tensor, $X_i -$ are body forces, $S_i -$ is the surface load, $\Sigma -$ is the surface of the volume *V*, consisting of two parts $\Sigma_1, \Sigma_2,$ $n_i -$ are the components of the outward normal to the surface $\Sigma,$ $\nu -$ is Poisson's ratio, and $\nabla^2 -$ is the Laplace operator.

It should be noted that condition (4) is obtained by considering the equilibrium equations on the boundary of the given domain. Equations (1)–(4) represent a boundary-value problem of elasticity theory formulated in terms of stresses.

In the boundary value problem (1–3), the number of equations is nine, namely, three equilibrium equations and six Beltrami–Michell equations. However, the strain compatibility conditions are not independent. In particular, the first group of three diagonal equations can be derived from the second group of non-diagonal equations by means of integral transformations. Therefore, when formulating the boundary value problem, it is sufficient to consider the second group of Beltrami–Michell equations corresponding to $i \neq j$.

Let us now consider the plane stress state in the absence of body forces. In this case, it is assumed that $\sigma_{33} = \sigma_{13} = \sigma_{23} = 0$, and the nonzero stress components σ_{11}, σ_{22} and

https://doi.org/10.3390/app16189303

$\sigma_{12} = \sigma_{21}$ are functions of the coordinates x and y. Under these assumptions, the equilibrium Equations (1) and the Beltrami–Michell Equations (2) take the following form:

$$\frac{\partial \sigma_{11}}{\partial x} + \frac{\partial \sigma_{12}}{\partial y} = 0, \qquad \frac{\partial \sigma_{21}}{\partial x} + \frac{\partial \sigma_{22}}{\partial y} = 0, \tag{5}$$

$$\nabla^2 \sigma_{12} + \frac{1}{1+\nu} \frac{\partial}{\partial x \partial y} (\sigma_{11} + \sigma_{22}) = 0. \tag{6}$$

The Beltrami–Michell Equations (6) depend on the second derivatives of the stress tensor components. Therefore, to form a consistent system of second-order differential equations, the equilibrium Equations (5) are differentiated with respect to the coordinates x and y, respectively. As a result, we obtain a system in terms of the components σ_{11}, σ_{22} and σ_{12} which will henceforth be referred to as problem A:

$$\frac{\partial^2 \sigma_{11}}{\partial x^2} + \frac{\partial^2 \sigma_{12}}{\partial x \partial y} = 0, \qquad \frac{\partial^2 \sigma_{21}}{\partial y \partial x} + \frac{\partial^2 \sigma_{22}}{\partial y^2} = 0, \tag{7}$$

$$\nabla^2 \sigma_{12} + \frac{1}{1+\nu} \frac{\partial}{\partial x \partial y} (\sigma_{11} + \sigma_{22}) = 0. \tag{8}$$

The boundary conditions on B have the following form

$$(\sigma_{11} n_1 + \sigma_{12} n_2)\big|_B = S_1, \quad (\sigma_{21} n_1 + \sigma_{22} n_2)\big|_B = S_2, \qquad \left(\frac{\partial \sigma_{11}}{\partial x} + \frac{\partial \sigma_{12}}{\partial y}\right)\bigg|_B = 0, \quad \left(\frac{\partial \sigma_{21}}{\partial x} + \frac{\partial \sigma_{22}}{\partial y}\right)\bigg|_B = 0. \tag{9}$$

The first boundary condition in (9) represents the condition for the surface force vector and relates the stress tensor components to the external load on the boundary of the domain. The second boundary condition is obtained from the equilibrium equations by considering them on the boundary of the given domain, and is used together with the differentiated system (7)–(8). Since the original equilibrium Equations (5) are differentiated in the construction of formulation A, retaining the original undifferentiated equilibrium conditions on the boundary prevents the appearance of arbitrary integration terms that do not satisfy the original equilibrium equations. Thus, conditions (9) ensure a consistent specification of the boundary data for the formulated problem A directly in terms of the stress tensor components.

Equations (7)–(9) represent a plane problem of elasticity theory formulated in terms of stresses. Such systems of equations can be solved numerically using finite difference methods on rectangular computational domains. In the case of complex domains, the application of the finite element method encounters difficulties associated with the transition to a variational problem, with the determination of a functional with respect to stresses corresponding to the original differential problem.

The application of the finite element method within the framework of the Galerkin method makes it possible to overcome the difficulties associated with the transition to a variational problem formulated with respect to stresses. Thus, the system of Equations (7)–(9) represents a plane boundary-value problem of elasticity theory with respect to the components of the stress tensor.

In the classical formulation, the solution of the plane problem of elasticity theory in terms of stresses is usually reduced to solving a biharmonic equation for the Airy stress function, which satisfies the equilibrium equations. In the present work, the boundary

https://doi.org/10.3390/app16189303

value problem is formulated directly in terms of the components of the tensor σ_{11}, σ_{22} and σ_{12} without using additional functions of the Airy type. This approach makes it possible to retain the stress tensor components as the primary unknowns in the subsequent construction of the variational formulation and the finite element approximation by the Galerkin method.

Further analysis of the Beltrami–Michell equations has shown that, under certain assumptions, they can be reduced to Poisson equations, which are efficient from the viewpoint of the numerical implementation of boundary-value problems formulated with respect to stresses. The following section is devoted to the discussion of this issue.

3. Stress-Based Poisson Equations

Let us consider the transformation of the Beltrami–Michell equations into a system of Poisson-type equations directly in terms of the stress tensor components. The basic idea of this transformation consists in using the equilibrium equations to eliminate the mixed derivatives of the stresses from the original Beltrami–Michell system. As a result, second-order differential equations with the Laplace operator can be obtained for the individual stress tensor components.

Let us consider the Beltrami–Michell Equations (2) in the case of a plane stress state, i.e.,

$$\begin{gathered}\frac{\partial^2\sigma_{11}}{\partial x^2}+\frac{\partial^2\sigma_{11}}{\partial y^2}+\frac{1}{1+\nu}\frac{\partial^2(\sigma_{11}+\sigma_{22})}{\partial x^2}=-2\frac{\partial X_1}{\partial x}-\frac{\nu}{1-\nu}(\frac{\partial X_1}{\partial x}+\frac{\partial X_2}{\partial y}),\\ \frac{\partial^2\sigma_{22}}{\partial y^2}+\frac{\partial^2\sigma_{22}}{\partial x^2}+\frac{1}{1+\nu}\frac{\partial^2(\sigma_{11}+\sigma_{22})}{\partial y^2}=-2\frac{\partial X_2}{\partial y}-\frac{\nu}{1-\nu}(\frac{\partial X_1}{\partial x}+\frac{\partial X_2}{\partial y}),\\ \frac{\partial^2\sigma_{12}}{\partial x^2}+\frac{\partial^2\sigma_{12}}{\partial y^2}+\frac{1}{1+\nu}\frac{\partial^2(\sigma_{11}+\sigma_{22})}{\partial x\partial y}=-(\frac{\partial X_1}{\partial y}+\frac{\partial X_2}{\partial x}).\end{gathered} \tag{10}$$

To transform system (10), we use the general form of the equilibrium Equations (1), which includes the body-force components X_1 and X_2. By differentiating the corresponding equilibrium equations with respect to the coordinates, we obtain relations between the second derivatives of the stress components and the derivatives of the body forces.

$$\begin{gathered}\frac{\partial^2\sigma_{11}}{\partial x\partial y}=-\frac{\partial^2\sigma_{12}}{\partial y^2}-\frac{\partial X_1}{\partial y},\\ \frac{\partial^2\sigma_{22}}{\partial y\partial x}=-\frac{\partial^2\sigma_{21}}{\partial x^2}-\frac{\partial X_2}{\partial x}.\end{gathered} \tag{11}$$

Adding the obtained relations (11) and grouping the derivatives of the stress components, we obtain an expression for the mixed derivative of the sum of the normal stresses:

$$\frac{\partial^2(\sigma_{11}+\sigma_{22})}{\partial x\partial y}=-\Delta\sigma_{12}-(\frac{\partial X_1}{\partial y}+\frac{\partial X_2}{\partial x}). \tag{12}$$

Substituting relation (12) into the third equation of the Beltrami–Michell system (10), we eliminate the mixed derivative of the sum $\sigma_{11}+\sigma_{22}$. After the corresponding transformations, we obtain a Poisson-type equation directly in terms of the shear stress component σ_{12}:

$$\Delta\sigma_{12}=-(\frac{\partial X_1}{\partial y}+\frac{\partial X_2}{\partial x}). \tag{13}$$

Substituting the obtained relation (13) into Equation (12) leads to the following condition for the sum of the normal stresses:

$$\frac{\partial^2(\sigma_{11}+\sigma_{22})}{\partial x\partial y}=0. \tag{14}$$

In the work of Timoshenko and Goodier [1], it is noted that stresses depend linearly on the coordinates. Apparently, this is related to the experimental fact that, for isotropic bodies undergoing elastic and plastic deformations, the relationship between the invariants of the stress tensor, $\sigma=\sigma_{11}+\sigma_{22}+\sigma_{33}$, and the strain tensor, $\theta=\varepsilon_{11}+\varepsilon_{22}+\varepsilon_{33}$, is linear, i.e., $\sigma=K\theta$ where $K=\lambda+2\mu/3.$ Taking into account that the strains depend on displacements belonging to the function class C^2, as solutions of the Navier equations, the linearity of $\sigma=\sigma_{11}+\sigma_{22}+\sigma_{33}$ becomes evident.

Taking into account the last relation (14), the original Beltrami–Michell system (10) can be transformed into a system of Poisson-type equations directly in terms of the components σ_{11}, σ_{22} and σ_{12}. The resulting formulation will henceforth be referred to as problem *B*.

$$\begin{gathered}\frac{\partial^2\sigma_{11}}{\partial x^2}+\frac{\partial^2\sigma_{11}}{\partial y^2}=-2\frac{\partial X_1}{\partial x}-\frac{\nu}{1-\nu}(\frac{\partial X_1}{\partial x}+\frac{\partial X_2}{\partial y}),\\ \frac{\partial^2\sigma_{22}}{\partial y^2}+\frac{\partial^2\sigma_{22}}{\partial x^2}=-2\frac{\partial X_2}{\partial y}-\frac{\nu}{1-\nu}(\frac{\partial X_1}{\partial x}+\frac{\partial X_2}{\partial y}),\\ \frac{\partial^2\sigma_{12}}{\partial x^2}+\frac{\partial^2\sigma_{12}}{\partial y^2}=-(\frac{\partial X_1}{\partial y}+\frac{\partial X_2}{\partial x}).\end{gathered} \tag{15}$$

Unlike problem *A*, where the Beltrami–Michell equations are used together with the differentiated equilibrium equation, in problem *B* the principal differential relations are represented as Poisson-type equations for the individual stress tensor components. Here, the equilibrium equations are used at the stage of transforming the original system and must be taken into account when forming consistent boundary conditions. This form is of particular interest for the subsequent construction of the weak formulation and the finite element approximation by the Galerkin method.

Let us now consider the possibility of a similar transformation of the Beltrami–Michell equations for the three-dimensional problem. Unlike the plane case considered above, it is further assumed that the body forces are potential and can be represented through a scalar potential φ [2], i.e.,

$$X_i=\varphi_{,i}. \tag{16}$$

Taking (16) into account, the original Beltrami–Michell equations for the three-dimensional case take the following form

$$\nabla^2\sigma_{ij}+\frac{1}{1+\nu}\sigma_{,ij}=-2\varphi_{,ij}-\frac{\nu}{1-\nu}\delta_{ij}\varphi_{,kk}. \tag{17}$$

Performing the corresponding contraction of Equation (17) over the repeated indices, we obtain a relation for the first invariant of the stress tensor:

$$\nabla^2\sigma=-\frac{1+\nu}{1-\nu}\nabla^2\varphi. \tag{18}$$

Following the work of Timoshenko and Goodier [1], the following relation can be obtained by equating the functions under the Laplace operators

$$\sigma=-\frac{1+\nu}{1-\nu}\varphi. \tag{19}$$

Substituting expression (19) into Equation (17) and taking into account the potential character of the body forces (16), and

$$\varphi_{,ij}=\frac{1}{2}(X_{i,j}+X_{j,i}), \tag{20}$$

we eliminate the first invariant of the stress tensor from the original system. After the transformations, we obtain a Poisson-type equation directly in terms of the stress tensor components:

$$\nabla^2\sigma_{ij} = -\frac{1-2\nu}{2(1-\nu)}(X_{i,j}+X_{j,i}) - \frac{\nu}{1-\nu}\delta_{ij}X_{k,k}. \tag{21}$$

According to (3) and (4), the following boundary conditions should be added to it:

$$\sigma_{ij}n_j\big|_{\Sigma_2} = S_i, \tag{22}$$

$$(\sigma_{ij}+X_i)\big|_{\Sigma} = 0. \tag{23}$$

Equations (21)–(23) form the three-dimensional boundary value formulation directly in terms of the stress tensor components, in which the principal differential Equation (21) has the structure of a Poisson equation. Thus, the paper considers two forms of the stress-based formulation: the original system, constructed on the basis of the Beltrami–Michell and equilibrium equations, and the transformed system of Poisson-type equations for the stress tensor components. In what follows, the corresponding weak forms and finite element schemes based on the Galerkin method are constructed for both formulations, which makes it possible to investigate them within a unified numerical approach.

4. The Galerkin Finite Element Method for Stresses

For the numerical solution of the plane boundary value problems *A* and *B* formulated above, we apply the finite element method based on the Galerkin approach. The computational domain $\Omega \subset R_2$ will be considered a bounded domain with a piecewise-smooth boundary *B*, on which the corresponding boundary conditions (9) are specified. The stress tensor components are directly considered as the primary unknowns. In operator form, problems *A* and *B* can be represented as follows:

$$L\sigma = F. \tag{24}$$

Here *L* denotes the differential operator corresponding to the stress-based formulation *A* or *B*, σ is the vector of independent stress tensor components $\sigma_{11}, \sigma_{22}, \sigma_{12}$, and $F-$ is the vector of right-hand sides, determined by the specified body forces and surface loads. This operator representation is used below to construct an approximate solution by the Galerkin method.

The approximate solution of problem (24) will be sought in a finite-dimensional space generated by a system of basis functions. For each sought stress component, the corresponding approximation is represented in the form:

$$\sigma = \sum_{i=1}^{n} a_i\varphi_i. \tag{25}$$

where φ_k are the basis functions of the chosen finite-dimensional space, and the expansion coefficients determine the approximate values of the sought stress components. The basis functions are chosen taking into account the finite element approximation used and the nature of the boundary conditions.

Substituting approximation (25) into the operator Equation (24), multiplying the residual by the corresponding basis functions, and requiring its orthogonality to the chosen finite-dimensional space, we obtain the system of Galerkin relations:

$$\int_\Omega L\sigma\cdot\varphi_i d\Omega = \int_\Omega F\cdot\varphi_i d\Omega, \quad i = 1,\ldots.n. \tag{26}$$

Relation (26) defines a finite-dimensional system for the coefficients of the approximate solution. The convergence of the Galerkin approximation is determined by the properties of the corresponding bilinear form, the choice of the finite-dimensional space, and the regularity of the solution. In the present work, the main emphasis is placed on constructing a discrete scheme directly in terms of the stress components and on its numerical verification on a problem with a known analytical solution.

Since the differential operators in the problems under consideration contain second derivatives of the stress components, direct use of relation (26) would require increased smoothness of the approximating functions. To reduce the order of the derivatives, integration by parts is performed, taking into account the corresponding boundary conditions. As a result, the differential formulation is reduced to the weak form:

$$a(\sigma,\varphi)=f. \tag{27}$$

where $a(\sigma,\varphi)$ denotes the bilinear form containing the stress components, their first derivatives, and the basis functions, and $f-$ is the corresponding linear functional, determined by the external loads and boundary data. The transition to the weak form makes it possible to use standard C^0- continuous finite element approximations.

For the finite element discretization, the domain Ω is divided into a set of triangular elements Ω_e. In the present work, linear Lagrange basis functions are used to approximate each stress tensor component. Within an individual finite element, the approximate stress field is represented through its nodal values and the corresponding shape functions. For a triangular element, the linear basis functions have the form:

$$\sigma=\sum_{i=1}^{l}N_i\sigma_i,$$

where N_e- is the number of nodes of the finite element. For a three-node triangular element, the linear basis functions can be written as [7]:

$$N_i(x,y)=\frac{1}{2A}(a_i+b_ix+c_iy),\quad i=1,..3. \tag{28}$$

In expression (28), A_e- denotes the area of the triangular finite element, and the coefficients of the basis functions $a_i,\ b_i,\ c_i$ are determined by the coordinates of its nodes. Using the same shape functions to approximate the components makes it possible to directly relate the unknown coefficients of the discrete problem to the nodal stress values σ_{11},σ_{22} and σ_{12}. The basis functions $N_i(x,y)$ play an important role in the construction of the local and global stiffness matrices.

To construct the local finite element system, the first equation of system (7) is multiplied by the basis function $[N]^T=[N_1,N_2,N_3]^T$ and integrated over the domain of an individual finite element Ω_e. After integration by parts and accounting for the corresponding boundary conditions, we obtain:

$$\begin{aligned}\int_{\Omega^e}[N]^T(\frac{\partial^2\sigma_{11}}{\partial x^2}+\frac{\partial^2\sigma_{12}}{\partial x\partial y})d\Omega&=\int_{\Omega}\left[\left\{\frac{\partial}{\partial x}(\frac{\partial\sigma_{11}}{\partial x}[N]^T)-\frac{\partial[N]^T}{\partial x}\frac{\partial\sigma_{11}}{\partial x}\right\}+\left\{\frac{\partial}{\partial y}(\frac{\partial\sigma_{12}}{\partial x}[N]^T)-\frac{\partial[N]^T}{\partial y}\frac{\partial\sigma_{12}}{\partial x}\right\}\right]d\Omega=\\&=\int_{\partial\Omega}\left(\frac{\partial N}{\partial x}[N]^T\{\sigma_{11}\}n_1+\frac{\partial N}{\partial x}[N]^T\{\sigma_{12}\}n_2\right)ds-\int_{\Omega}\left(\frac{\partial[N]^T}{\partial x}\frac{\partial\sigma_{11}}{\partial x}+\frac{\partial[N]^T}{\partial y}\frac{\partial\sigma_{12}}{\partial x}\right)d\Omega=0.\end{aligned} \tag{29}$$

Substituting the linear basis functions (28) into the variational relation (29) and taking into account the boundary conditions (9), we obtain the discrete equation for the corresponding nodal values of the stress tensor components:

$$\left(\frac{\partial[N]^T}{\partial x}\frac{\partial N}{\partial x}\{\sigma_{11}\}+\frac{\partial[N]^T}{\partial y}\frac{\partial N}{\partial x}\{\sigma_{12}\}\right)A=\int_{\partial\Omega}S_1[N]^T\frac{\partial N}{\partial x}ds. \tag{30}$$

Similarly, applying the Galerkin procedure to the second equation of system (7) and to Equation (8), we obtain two more local relations

$$\left(\frac{\partial[N]^T}{\partial x}\frac{\partial N}{\partial y}\{\sigma_{21}\}+\frac{\partial[N]^T}{\partial y}\frac{\partial N}{\partial y}\{\sigma_{22}\}\right)A=\int_{\partial\Omega}S_2[N]^T\frac{\partial N}{\partial y}ds, \tag{31}$$

$$\begin{gathered}\left(\left(\frac{\partial[N]^T}{\partial x}\frac{\partial N}{\partial x}+\frac{\partial[N]^T}{\partial y}\frac{\partial N}{\partial y}\right)\{\sigma_{12}\}+\frac{1}{1+\nu}\frac{\partial[N]^T}{\partial y}\frac{\partial N}{\partial x}\{\sigma_{11}\}+\frac{1}{1+\nu}\frac{\partial[N]^T}{\partial x}\frac{\partial N}{\partial y}\{\sigma_{22}\}\right)A= \\ =\frac{\nu}{1+\nu}\int_{\partial\Omega}[N]^T\frac{\partial N}{\partial x}\{\sigma_{12}\}n_1ds+\frac{\nu}{1+\nu}\int_{\partial\Omega}[N]^T\frac{\partial N}{\partial y}\{\sigma_{12}\}n_2ds.\end{gathered} \tag{32}$$

The obtained local Equations (30)–(32) are combined into the matrix system of the finite element:

$$K\sigma=F. \tag{33}$$

where

$$K^{(e)}=\begin{bmatrix}K^{ii} & K^{ij} & K^{ik}\\ K^{ji} & K^{jj} & K^{jk}\\ K^{ki} & K^{kj} & K^{kk}\end{bmatrix},\ \sigma=\left[\sigma_{11}^m,\quad \sigma_{22}^m,\quad \sigma_{12}^m\right]^T,\ F=\left[f_1^m,\quad f_2^m,\quad f_3^m\right]^T. \tag{34}$$

$$K^{mn}=\begin{bmatrix}k_{11}^{mn} & k_{12}^{mn} & k_{13}^{mn}\\ k_{21}^{mn} & k_{22}^{mn} & k_{23}^{mn}\\ k_{31}^{mn} & k_{32}^{mn} & k_{33}^{mn}\end{bmatrix},\ m,n\in\{i,j,k\},$$

$$k_{11}^{mn}=\frac{\partial N_m}{\partial x}\frac{\partial N_n}{\partial x}A,\qquad k_{12}^{mn}=0,\qquad k_{13}^{mn}=\frac{\partial N_m}{\partial y}\frac{\partial N_n}{\partial x}A,$$

$$k_{21}^{mn}=0,\qquad k_{22}^{mn}=\frac{\partial N_m}{\partial y}\frac{\partial N_n}{\partial y}A,\qquad k_{23}^{mn}=\frac{\partial N_m}{\partial x}\frac{\partial N_n}{\partial y}A,$$

$$k_{31}^{mn}=\frac{1}{1+\nu}\frac{\partial N_m}{\partial y}\frac{\partial N_n}{\partial x}A,\quad k_{32}^{mn}=\frac{1}{1+\nu}\frac{\partial N_m}{\partial x}\frac{\partial N_n}{\partial y}A,\quad k_{33}^{mn}=\left(\frac{\partial N_m}{\partial x}\frac{\partial N_n}{\partial x}+\frac{\partial N_m}{\partial y}\frac{\partial N_n}{\partial y}\right)A.$$

$$\begin{gathered}f_1^m=\int_{\partial\Omega}\frac{\partial N}{\partial x}[N]^TS_1ds,\quad f_2^m=\int_{\partial\Omega}\frac{\partial N}{\partial y}[N]^TS_2ds,\\ f_3^m=\frac{\nu}{1+\nu}\int_{\partial\Omega}\frac{\partial N}{\partial x}[N]^T\{\sigma_{12}\}n_1ds+\frac{\nu}{1+\nu}\int_{\partial\Omega}\frac{\partial N}{\partial y}[N]^T\{\sigma_{12}\}n_2ds.\end{gathered} \tag{35}$$

In system (33), K_e represents the local finite element matrix, $\sigma_e -$ is the vector of nodal values of the stress tensor components, and $F_e -$ is the local right-hand-side vector, formed taking into account the specified loads and boundary conditions. The elements of the matrix K_e are determined by integrals of the products of the derivatives of the basis functions in accordance with the variational formulation of the problem.

After the standard assembly procedure for the local matrices and vectors, the global system of linear algebraic equations is formed directly in terms of the nodal values σ_{11},σ_{22} and σ_{12}. After imposing the corresponding boundary conditions, the resulting system is solved numerically. In the developed implementation, Gaussian elimination is used to solve the global system.

A similar procedure is applied to problem *B*, formulated on the basis of the Poisson-type Equation (15). After multiplying each equation by the corresponding basis function and integrating by parts, a weak formulation is obtained, and the subsequent approximation with linear triangular elements leads to local and global systems directly in terms of the nodal values of the stress tensor components. Thus, problems *A* and *B* are implemented within a unified Galerkin finite element approach.

In the numerical solution of problems of applied mechanics, it is appropriate to use the FreeFEM++ programming language, which is designed for solving differential equations by the finite element method. FreeFEM++ is based on the C++ programming language supplemented with finite element method algorithms. To solve differential equations numerically in FreeFEM++, it is first necessary to pass from the differential problem to the variational formulation and to construct the corresponding functional. In FreeFEM++, this functional must be specified in bilinear form using the Galerkin method.

5. Numerical Validation and Convergence Analysis for the Kirsch Problem

For the numerical verification of the developed stress formulations and the constructed finite element schemes, we consider the classical Kirsch problem of a stretched elastic plate with a circular hole. The choice of this problem is motivated by the availability of a known analytical solution and the pronounced stress concentration in the vicinity of the hole boundary, which makes it possible to quantitatively assess the ability of the proposed method to reproduce local features of the stress state. The numerical results for Problems A and B are subsequently compared with the analytical solution and with each other.

5.1. Problem Definition and Analytical Reference Solution

A rectangular elastic plate of dimensions $2lx2h$ with a central circular hole of radius $a-$ is considered. A uniformly distributed tensile load of intensity $S-$ is applied along the *OX* axis to two opposite outer boundaries of the plate, while the boundary of the hole is assumed to be free of external forces. The plate material is assumed to be homogeneous, isotropic, and linearly elastic. The objective is to determine the distribution of the components of the stress tensor in the plate domain, including the region of local stress concentration around the hole.

$$l = 2\text{cm}, \quad h = 2\text{cm}, \quad a = 0.2\text{cm}.$$

It should be noted that the analytical Kirsch solution used corresponds to an infinite elastic plane with a circular hole, whereas the numerical model is considered within a finite computational domain. Therefore, the difference between the analytical and numerical values may include not only the finite element discretization error but also the effect of the finite distance from the hole to the outer boundary.

$$\begin{array}{lll} x = \pm l: & \sigma_{11} = S, & \sigma_{12} = 0, \\ y = \pm h: & \sigma_{22} = 0, & \sigma_{12} = 0, \\ r = a: & \sigma_{rr}(r = a, \theta) = 0, & \sigma_{r\theta}(r = a, \theta) = 0. \end{array} \tag{36}$$

where $\theta-$ is the angle, $a-$ is the radius of the hole, and $S = 1$. In the numerical calculations, normalization with respect to the magnitude of the applied stress is used, and $S = 1$ is assumed. Therefore, all subsequently presented stress values can be interpreted in dimensionless form as σ_{ij} / S.

The analytical solution of the Kirsch problem, used below as a reference solution for evaluating the numerical results, can be expressed in polar coordinates in the following form (Figure 1).

$$\begin{aligned} \sigma_{11} &= S\left[1 - \frac{r^2}{a^2}\left(\frac{3}{2}\cos 2\theta + \cos 4\theta\right) + \frac{3r^4}{2a^4}\cos 4\theta\right], \\ \sigma_{22} &= -S\left[\frac{r^2}{a^2}\left(\frac{1}{2}\cos 2\theta - \cos 4\theta\right) + \frac{3r^4}{2a^4}\cos 4\theta\right], \\ \sigma_{12} &= -\frac{S}{2}\left[\frac{r^2}{a^2}\left(\sin 2\theta + 2\sin 4\theta\right) - \frac{3r^4}{2a^4}\sin 4\theta\right]. \end{aligned} \tag{37}$$

where $a-$ is the radius of the circular hole, $r-$ is the radial distance from the center of the hole to the considered point *M*, $\theta-$ is the polar angle measured from the positive *x*-

axis, and S is the magnitude of the uniformly distributed tensile stress applied along the opposite sides of the plate.

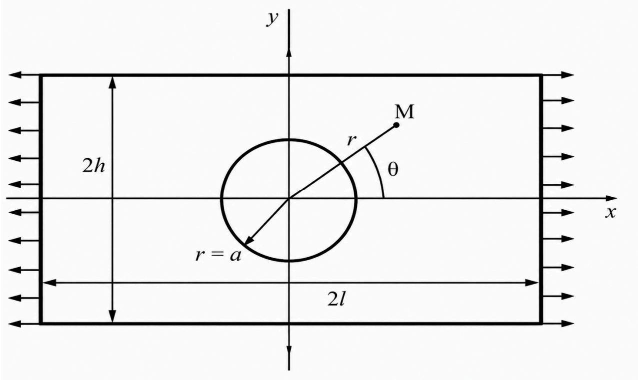

Figure 1. Geometry and loading conditions for the Kirsch problem.

5.2. Finite Element Discretization and Numerical Implementation

The computational domain is discretized using triangular finite elements. To improve the accuracy of determining local stress gradients, the mesh is refined in the vicinity of the circular hole, where the maximum stress concentration is expected (Figure 2). The nodal coordinates and mesh topology generated in FreeFEM++ are also used in the developed C++ program, allowing the results to be compared on the same computational geometry.

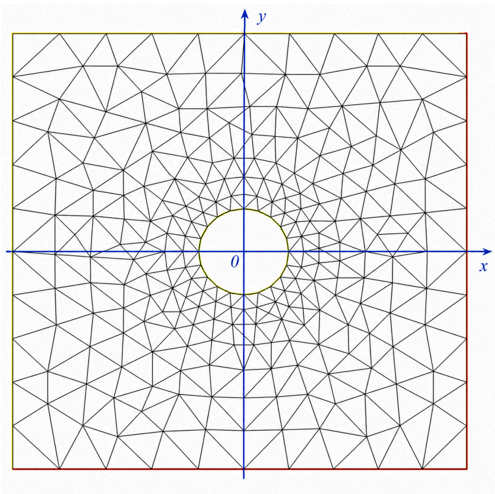

Figure 2. Finite element mesh of the plate with a central circular hole, refined in the vicinity of the hole.

After assembling the local finite element matrices, a global system of linear algebraic equations is formed with respect to the nodal values of the stress components. The resulting system is solved using the developed C++ program. An independent implementation of both stress formulations is also carried out in FreeFEM++, which is used for additional verification of the numerical results.

5.3. Comparison of Stress Distributions

Figure 3 presents the distributions of the normal stress component σ_{11} obtained using four approaches: (a) the developed Galerkin finite element scheme in C++; (b) the implementation of Problem A in FreeFEM++; (c) the implementation of Problem B based on Poisson-type equations in FreeFEM++; and (d) the analytical Kirsch solution (37).

https://doi.org/10.3390/app16189303

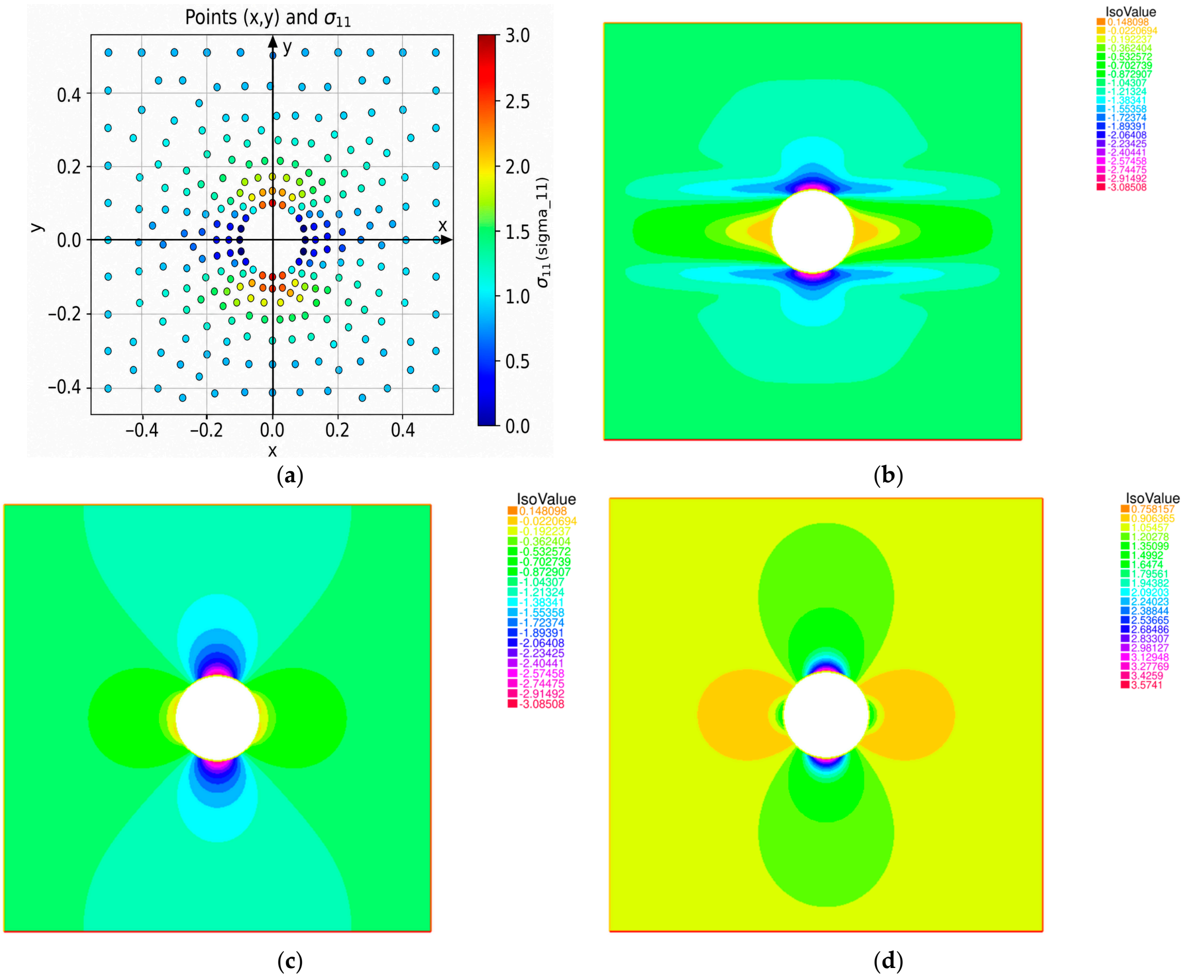

Figure 3. Distribution of σ_{11}: (**a**) Galerkin FEM implemented in C++; (**b**) formulation A implemented in FreeFEM++; (**c**) formulation B implemented in FreeFEM++; (**d**) analytical Kirsch solution.

In all four solutions, a characteristic concentration of the σ_{11} component near the upper and lower points of the hole is observed for the Kirsch problem. The maximum value reaches approximately *3S*, which corresponds to the well-known stress concentration factor for a circular hole under uniaxial tension. As the distance from the hole increases, the values of σ_{11} tend toward the applied stress *S*. Overall, the numerical distributions reproduce the characteristic behavior of the analytical solution, although for formulation *B*, a somewhat slower approach to the far-field stress state is noticeable in the transition region.

The distribution of the σ_{22} component is also characterized by pronounced localization near the hole boundary. All the considered solutions reproduce the same spatial structure of the stress field and the change in the sign of σ_{22} at different sections of the circular boundary. Quantitative differences between the individual formulations are most noticeable in the immediate vicinity of the hole, whereas away from the stress concentrator, the values of σ_{22} tend toward zero (Figure 4).

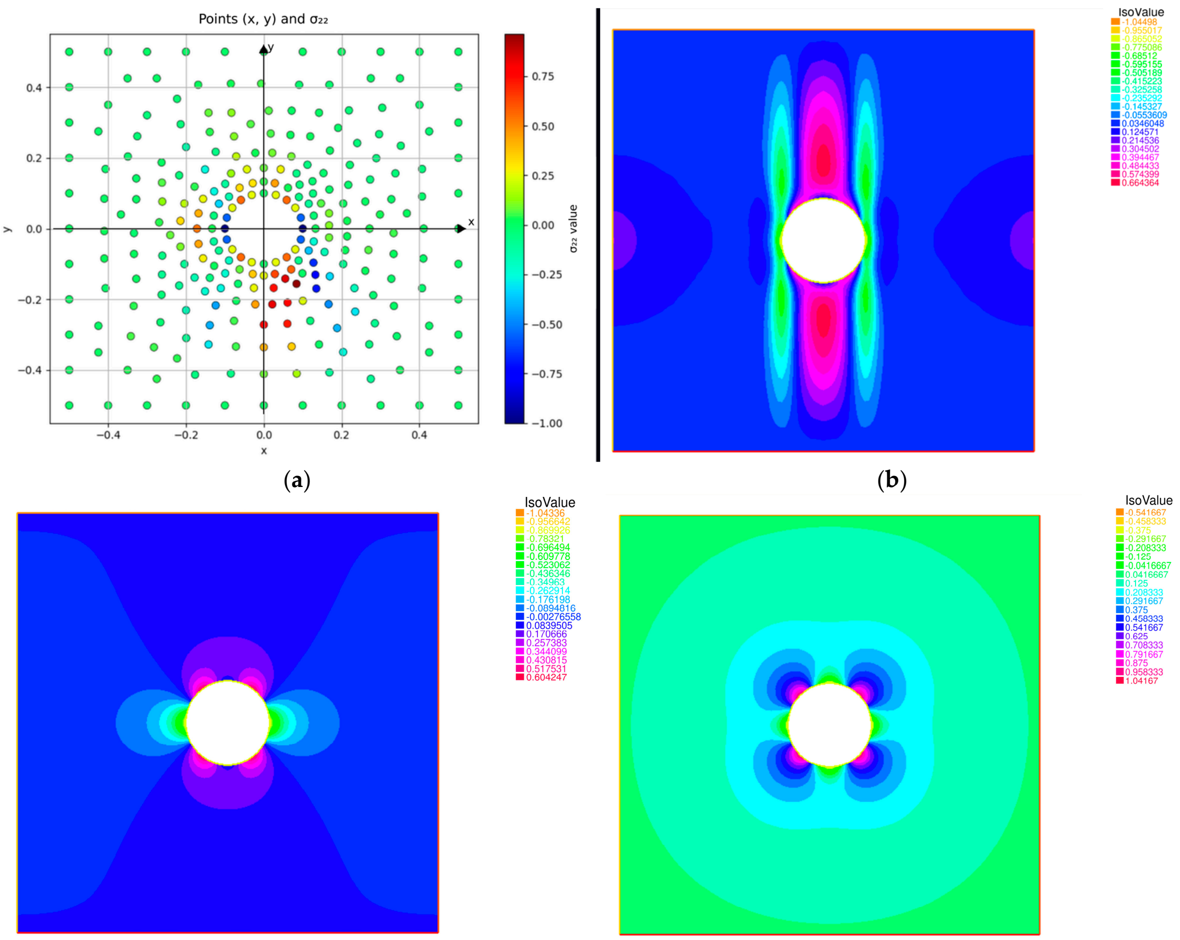

(**a**) (**b**)

(**c**) (**d**)

Figure 4. Distribution of σ_{22}: (**a**) Galerkin FEM implemented in C++; (**b**) formulation A implemented in FreeFEM++; (**c**) formulation B implemented in FreeFEM++; (**d**) analytical Kirsch solution.

For the shear component σ_{12}, the expected antisymmetric distribution with respect to the coordinate axes is preserved in all cases. The extreme values are localized near the hole boundary, while σ_{12} tends to zero with increasing distance from the hole. The largest differences between the numerical and analytical solutions are observed in regions of maximum stress gradients, associated with the increased sensitivity of the local field to spatial discretization (Figure 5).

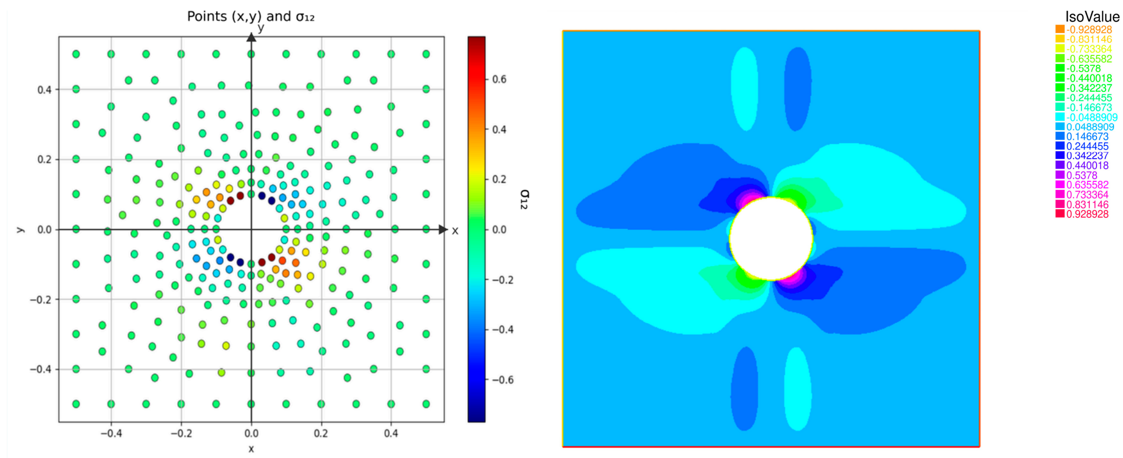

(**a**) (**b**)

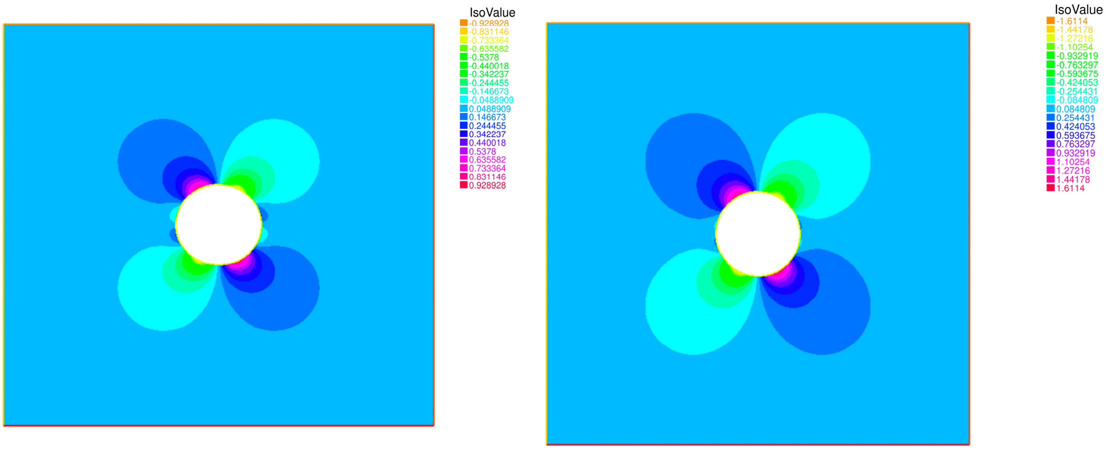

(**c**) (**d**)

Figure 5. Distribution of σ_{12} : (**a**) Galerkin FEM implemented in C++; (**b**) formulation A implemented in FreeFEM++; (**c**) formulation B implemented in FreeFEM++; (**d**) analytical Kirsch solution.

5.4. Quantitative Comparison Along Characteristic Sections

For a more detailed quantitative assessment of the obtained solutions, we consider the variation in the normalized stress component σ_{11} / S along characteristic sections of the plate. This representation allows the numerical and analytical results to be compared not only in terms of the overall structure of the stress field, but also in terms of the variation in the stress values near the stress concentrator and with increasing distance from the hole boundary.

Figure 6 presents the distribution of σ_{11} / S along the *OY* axis at $x = 0$, starting from the hole boundary and extending toward the outer boundary of the computational domain. In the immediate vicinity of the hole, the normal stress reaches its maximum value due to the stress concentration effect. As the distance from the hole increases, the value of σ_{11} / S decreases and gradually approaches the far-field stress level. The numerical solution obtained using the Poisson-type stress formulation reproduces the characteristic variation of the analytical Kirsch solution, with the most noticeable differences occurring in the region of increased stress gradient near the hole boundary.

For an additional assessment of the solution behavior, the variation in the normalized stress component σ_{11} / S along the *OX* axis on the central line of the plate was also considered. The corresponding results are presented in Figure 7. In this section, the stress variation is likewise governed by the influence of the circular hole: the greatest deviation from the far-field stress state is observed near its boundary, whereas with increasing *x*-coordinate, the influence of the stress concentrator gradually decreases. The obtained numerical values demonstrate good qualitative agreement with the analytical solution and correctly reproduce the characteristic stress redistribution along the considered section.

https://doi.org/10.3390/app16189303

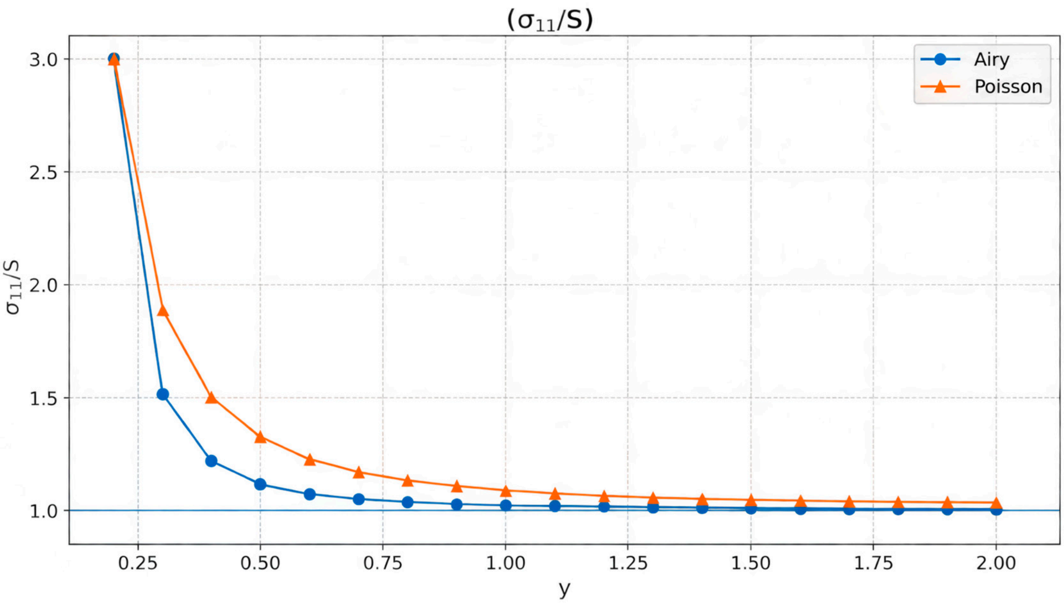

Figure 6. Comparison of normalized stress σ_{11}/S along the *OY* axis.

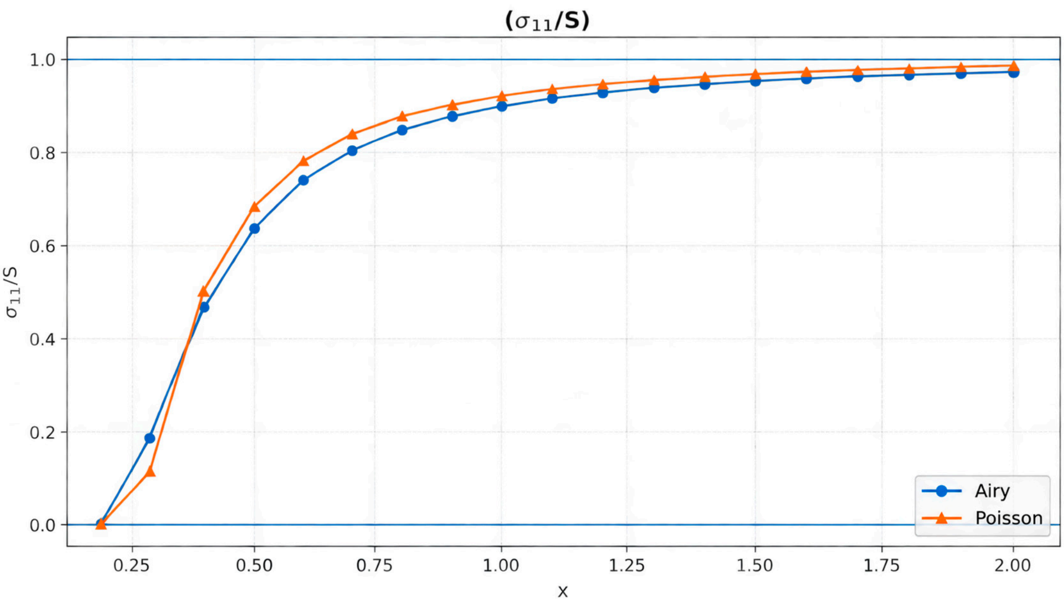

Figure 7. Comparison of normalized stress σ_{11}/S along the *OX* axis.

Comparison of the results along the two characteristic directions shows that the proposed stress formulation reproduces both the local variation of σ_{11} near the hole and the subsequent convergence of the solution to the far-field stress state. The largest discrepancies from the analytical solution are concentrated in regions of high stress gradients, indicating the need for further analysis of the influence of spatial discretization. Therefore, the accuracy of the numerical solution is subsequently assessed through successive refinement of the finite element mesh and analysis of the corresponding errors.

5.5. Mesh Refinement and Error Analysis

To quantitatively assess the accuracy of the developed finite element schemes, an error analysis was performed under successive refinement of the computational mesh. The analytical solution of the Kirsch problem (37), obtained based on the Airy stress function, was used as the reference solution. Calculations were performed for several values

https://doi.org/10.3390/app16189303

of the characteristic finite element size h. For each mesh, the maximum absolute error, mean absolute error, relative error, and observed convergence order p were determined.

To ensure the reproducibility of the calculations, Table 1 presents the main characteristics of the finite element meshes used in the convergence study, including the characteristic element size h the number of nodes, the number of triangular finite elements, and the total number of degrees of freedom.

Table 1. Characteristics of the finite element meshes used in the mesh-refinement study.

h	Number of Nodes	Number of Triangular Elements	Number of Degrees of Freedom
0.10	1250	2306	3590
0.05	3899	6434	11,377
0.0125	17,957	27,190	52,671

First, we consider the results for Problem A, based on the Beltrami–Michell equations. The obtained error characteristics under successive finite element mesh refinement are presented in Table 2.

Table 2. Error and convergence characteristics for formulation A based on the Beltrami–Michell equations.

h (Characteristic Element Size)	Max Absolute Error	Mean Absolute Error	Relative Error (%)	Convergence Order (p)
0.10	0.498	0.0614	10.367	—
0.05	0.410	0.0596	9.163	0.18
0.0125	0.139	0.0251	3.189	0.76

As shown in Table 2, refinement of the finite element mesh is accompanied by a consistent decrease in both the maximum and mean absolute errors. The maximum absolute error decreases from 0.498 at $h = 0.10$ to 0.139 at $h = 0.0125$, while the mean absolute error decreases from 0.0614 to 0.0251. At the same time, the relative error decreases from 10.367% to 3.189%, indicating improved agreement between the numerical solution and the analytical Kirsch solution with increasing spatial mesh resolution.

The observed convergence order is $p = 0.18$ and $p = 0.76$ for successive refinement levels. Since the values of p vary and do not reach a constant asymptotic level, they should be regarded as numerical estimates of the error reduction rate for the investigated meshes rather than as the theoretical convergence order of the finite element scheme.

A similar analysis was performed for Problem B, formulated based on Poisson-type equations directly in terms of the components of the stress tensor. To ensure comparability of the results, the same characteristic finite element sizes and the same error measures were used. The results are presented in Table 3.

Table 3. Error and convergence characteristics for formulation B based on the stress Poisson equations.

h (Characteristic Element Size)	Max Absolute Error	Mean Absolute Error	Relative Error (%)	Convergence Order (p)
0.10	0.376	0.092	10.671	—
0.05	0.282	0.075	8.583	0.314
0.0125	0.262	0.0667	7.415	0.106

The results presented in Table 3 also show a reduction in the error with refinement of the finite element mesh. The maximum absolute error decreases from *0.376* at $h = 0.10$

to 0.262 at h = 0.0125, while the mean absolute error decreases from 0.092 to 0.0667. The relative error decreases from 10.671% to 7.415%. Thus, for Problem B, a consistent convergence of the numerical solution toward the analytical solution is also observed as the characteristic finite element size decreases.

The observed convergence orders are p = 0.314 and p = 0.106. As in the case of Problem A, they do not form a constant sequence corresponding to an established asymptotic regime. Therefore, these values characterize the numerical behavior of the scheme only within the considered range of meshes.

A comparison of the results in Tables 2 and 3 shows that, for both stress formulations, a decrease in the finite element size is accompanied by a reduction in the considered error measures. At the same time, the rate of error reduction differs. On the finest mesh considered, with h = 0.0125, the relative error for Problem A is 3.189%, whereas for Problem B it is *7.415*%. Thus, within the numerical experiment performed, formulation A demonstrates closer agreement with the analytical Kirsch solution.

5.6. Comparison with the Standard Displacement-Based Finite Element Formulation

For an additional assessment of the developed stress-based formulations, the Kirsch problem was also solved using the standard displacement-based finite element formulation. In contrast to formulations A and B, where the components of the stress tensor are the primary unknown functions, in the classical formulation the unknowns are the displacement vector components u_1 and u_2. After determining the displacement field, the strain components are calculated by differentiating the finite element approximation, and the corresponding stress components are recovered using the constitutive relations of linear elasticity.

To ensure a correct comparison, the same geometric parameters of the plate and circular hole, material properties, and external loading were used in all three calculations. In addition, the same or the closest possible mesh resolution was employed for the comparative analysis. This reduces the influence of differences associated with geometry, loading, and discretization and allows the comparison to focus directly on the method used to determine the stress components.

In the standard displacement-based formulation, the approximate field is represented as:

$$u_i^h(x,y) = \sum_{k=1}^{N} N_k(x,y) u_i^{(k)}, \quad i = 1,2.$$

where $N_k(x,y) -$ are the finite element basis functions, and $u_i^{(k)} -$ are the nodal values of the displacement components. After solving the global system of finite element equations, the strain components are determined from the kinematic relations.

$$\varepsilon_{11} = \frac{\partial u_1}{\partial x}, \quad \varepsilon_{22} = \frac{\partial u_2}{\partial y},$$
$$\varepsilon_{12} = \frac{1}{2}\left(\frac{\partial u_1}{\partial y} + \frac{\partial u_2}{\partial x}\right).$$

The corresponding stress components are then calculated from Hooke's law for the plane stress state considered. Thus, in the displacement-based formulation, the stresses are derived quantities obtained after computing and differentiating the displacement field, whereas in formulations *A* and *B* they are determined directly as the primary unknowns of the finite element system.

For the quantitative comparison, the same error measures as those used in the analysis of formulations A and B were employed: the maximum absolute error, the mean absolute error, and the relative error with respect to the analytical Kirsch solution. The results for the finest mesh considered are presented in Table 4.

Table 4. Comparison of the stress-based and displacement-based finite element formulations for the Kirsch problem.

Formulation	Maximum Absolute Error	Mean Absolute Error	Relative Error, %
Formulation A (h = 0.0125)	0.139	0.0251	3.189
Formulation B (h = 0.0125)	0.262	0.0667	7.415
Standard displacement-based FEM (h = 0.0125)	0.140	0.064474	7.165

As shown in Table 4, all three finite element formulations reproduce the characteristic stress distribution in a plate with a circular hole and allow the stress distribution near the hole boundary to be described. The results obtained using the standard displacement-based formulation are also consistent with the analytical Kirsch solution, which confirms the correctness of the stress-based equations used and the solution method within the Galerkin finite element framework.

In the classical finite element formulation, the stress components are determined at the post-processing stage from the gradients of the computed displacement field. In the proposed formulations A and B, the corresponding stress components are included directly among the primary unknowns of the discrete problem. Therefore, the comparison makes it possible to assess not only the agreement between different computational implementations but also the features of directly determining the stresses compared with their recovery from the displacement field.

For the problem considered and the selected mesh, the relative error of the standard displacement-based formulation was 7.165%, whereas for formulations A and B it was 3.189% and 7.415%, respectively. These results show that the direct stress-based approximation is capable of reproducing the local stress field in the vicinity of the stress concentrator with an accuracy comparable to that of the classical finite element formulation.

The comparison was performed for the specific Kirsch problem, the selected type of linear triangular finite elements, and the considered sequence of computational meshes. In addition, the largest errors occur in the vicinity of the circular hole, where the stress field is characterized by high spatial gradients and increased sensitivity to discretization.

Overall, the analysis demonstrates a reduction in the discrepancy between the numerical and analytical solutions with mesh refinement for both formulations considered. The results also indicate the desirability of further investigating the influence of local mesh refinement and higher-order finite elements on the accuracy of the direct determination of the components of the stress tensor.

6. Discussion

In the present work, two finite element formulations of a boundary value problem in linear elasticity are investigated, in which the components of the stress tensor are considered directly as the primary unknown functions. Formulation A is based on the combined use of the equilibrium equations and the Beltrami–Michell equations, whereas formulation B is obtained by transforming the original system into Poisson-type equations for the individual components of the stress tensor. For both formulations, weak forms are constructed using the Galerkin method, and finite element discretization is performed using continuous linear basis functions on triangular elements. As a result, the unknowns of the corresponding global systems are directly the nodal values of the stress components, without the preliminary determination of the displacement field.

https://doi.org/10.3390/app16189303

The numerical results for the Kirsch problem show that both developed formulations reproduce the characteristic stress distribution in a plate with a circular hole, including the region of pronounced stress concentration near the hole boundary. Comparison with the analytical solution shows a consistent decrease in the considered error measures as the finite element mesh is refined. On the finest mesh considered, with a characteristic size of h = 0.0125, the relative error was 3.189% for formulation *A* and 7.415% for formulation *B*. These results confirm the applicability of both stress-based formulations to the considered benchmark problem and demonstrate the possibility of directly determining the stress tensor components within the finite element method.

The additional comparison with the standard displacement-based finite element formulation allows the obtained results to be considered not only as a mutual verification of two independent implementations of the stress-based schemes. In the classical displacement-based formulation, the displacement components are the primary unknowns, while the strains and stresses are determined after solving the problem by differentiating the finite element approximation of the displacement field and applying the constitutive relations. In formulations A and B, in contrast, the stress components are included directly among the primary unknowns of the discrete system. The comparison, performed using the same geometric parameters, material properties, loading, and comparable mesh resolution, makes it possible to directly assess the features of these two approaches to the numerical determination of the stress field. For the standard displacement-based finite element formulation, the maximum absolute, mean absolute, and relative errors were 0.140, 0.064474, and 7.165%, respectively. For the discretization considered, these results show that formulation A provides the closest agreement with the analytical solution, whereas the standard displacement-based formulation and formulation B demonstrate comparable levels of error.

When interpreting the quantitative comparison with the analytical solution, the specific feature of the selected benchmark problem should also be taken into account. The classical Kirsch solution corresponds to an infinite elastic plane with a circular hole, whereas the finite element model is considered within a finite computational domain. Consequently, the discrepancy between the analytical and numerical values may be determined not only by the spatial discretization error but also by the influence of the finite distance from the hole to the outer boundaries of the computational domain. For this reason, the geometric dimensions l and h, the hole radius a, and the dimensionless ratio a/L specified in the problem formulation are essential for interpreting the obtained errors. In particular, the residual discrepancy with the Kirsch solution under mesh refinement should not automatically be attributed exclusively to the finite element approximation error.

The independent implementation of the developed schemes in a custom C++ program and in FreeFEM++ provides an additional verification of the correctness of the derived weak forms, finite element discretization, and computational algorithm. The agreement between the results of the two implementations reduces the likelihood that the observed numerical behavior is associated with the specific features of a particular program code.

The present study has several limitations that define the scope of applicability of the obtained results. First, the numerical implementation and verification were performed for two-dimensional linear isotropic elasticity under small deformations. Therefore, the obtained results should not be directly extended to anisotropic materials, nonlinear constitutive relations, elastoplastic processes, large deformations, crack formation, or other physically or geometrically nonlinear problems without additional theoretical and numerical investigation. The present work considers the basic linear formulation required to verify the feasibility of a direct finite element approximation of the stress components within the proposed Galerkin scheme.

The second limitation is related to the spatial discretization used. In both formulations, linear basis functions on triangular finite elements are employed. This approximation is convenient for the construction and verification of the proposed scheme; however, its accuracy may decrease in regions with high stress gradients, particularly in the immediate vicinity of a stress concentrator. The reduction in error observed with mesh refinement demonstrates the effectiveness of locally increasing the spatial resolution; however, for a more accurate representation of stresses in regions of stress concentration, higher-order finite elements and adaptive local mesh refinement should be investigated.

In addition, the finite element implementation performed in this study is limited to two-dimensional problems. Although the governing relations of elasticity can be formulated in three-dimensional form, the direct extension of the developed discrete scheme to three-dimensional problems requires a separate investigation. In particular, the corresponding three-dimensional weak forms must be constructed, the structure of the local and global finite element systems must be determined, and their systematic numerical verification must be performed using three-dimensional benchmark problems with known or independently obtained solutions. Therefore, the development and verification of a three-dimensional version of the method are considered a separate direction for future research.

Thus, the analysis shows that both stress-based formulations considered can be implemented using the Galerkin method and allow the stress tensor components to be determined directly at the nodes of the finite element mesh. The results obtained for the Kirsch problem confirm the applicability of the proposed approach to solving elasticity problems in terms of stresses.

At the same time, the identified differences between formulations A and B, the influence of spatial discretization, and the noted limitations define the directions for further development of the method, including the extension of the set of benchmark problems, the use of higher-order elements and adaptive meshes, as well as the development and verification of a three-dimensional stress-based finite element formulation.

7. Conclusions

In this study, two stress-based finite element formulations for two-dimensional linear elasticity were developed and investigated. Formulation *A* combines the Beltrami–Michell equations with the differentiated equilibrium equations, whereas formulation *B* is based on a transformed system of Poisson-type equations for the stress components. For both formulations, Galerkin weak forms were constructed and discretized using linear triangular finite elements, with the stress components treated directly as the primary nodal unknowns without preliminary computation of the displacement field.

The formulations were verified using the Kirsch problem and independent implementations in C++ and FreeFEM++. Both formulations reproduced the characteristic stress distribution and stress concentration near the circular hole. Mesh refinement reduced the relative error from 10.367% to 3.189% for formulation *A* and from 10.671% to 7.415% for formulation *B*. On the finest mesh considered, formulation A showed closer agreement with the analytical Kirsch solution.

The results demonstrate that the stress tensor components can be used directly as the primary unknowns in a Galerkin finite element formulation. The comparison with the analytical solution and the agreement between the two independent implementations support the applicability of the proposed formulations to the considered two-dimensional linear elasticity problem.

The present study is limited to two-dimensional linear isotropic elasticity and linear triangular elements. Further work will consider higher-order elements, adaptive mesh refinement in regions of stress concentration, three-dimensional formulations, and extensions to more general material models.

Author Contributions: Conceptualization, A.A.K.; Methodology, U.Z.D.; Software, A.A.B.; Validation, O.U.T.; Formal Analysis, U.Z.D.; Investigation, S.P.P.; Data Curation, M.N.A.; Writing—Original Draft, U.Z.D.; Writing—Review and Editing, U.Z.D.; Visualization, F.S.O.; Supervision, A.A.K. and U.Z.D. All authors have read and agreed to the published version of the manuscript.

Funding: This research received no external funding.

Institutional Review Board Statement: Not applicable.

Informed Consent Statement: Not applicable.

Data Availability Statement: The original contributions presented in this study are included in the article. Further inquiries can be directed to the corresponding author.

Conflicts of Interest: The authors declare no conflicts of interest.

References

1. Timoshenko, S.P.; Goodier, J.N. *Theory of Elasticity*, 3rd ed.; McGraw-Hill: New York, NY, USA, 1970; 567p.
2. Nowacki, W. *Theory of Elasticity*; Mir Publishers: Moscow, Russia, 1975; 872p.
3. Lurie, A.I.; Belyaev, A. *Theory of Elasticity*; Springer: Berlin/Heidelberg, Germany, 2005; 1050p. https://doi.org/10.1007/978-3-540-26455-2.
4. Sadd, M.H. *Elasticity: Theory, Applications, and Numerics*, 4th ed.; Academic Press: London, UK, 2020; 624p. https://doi.org/10.1016/C2017-0-03720-5.
5. Eslami, M.R.; Hetnarski, R.B.; Ignaczak, J.; Noda, N.; Sumi, N.; Tanigawa, Y. *Theory of Elasticity and Thermal Stresses: Explanations, Problems and Solutions*; Springer: Dordrecht, The Netherlands, 2013; 789p. https://doi.org/10.1007/978-94-007-6356-2.
6. Zienkiewicz, O.C.; Taylor, R.L.; Zhu, J.Z. *The Finite Element Method: Its Basis and Fundamentals*, 7th ed.; Butterworth-Heinemann: Oxford, UK, 2013; 714p. https://doi.org/10.1016/C2009-0-24909-9.
7. Desai, Y.M.; Eldho, T.I.; Shah, A.H. *Finite Element Method with Applications in Engineering*; Pearson Education: New Delhi, India, 2011; 492p.
8. Rektorys, K. *Variational Methods in Mathematics, Science and Engineering*, 2nd ed.; D. Reidel Publishing Company: Dordrecht, The Netherlands, 1980; 551p.
9. Kucher, V.A.; Markenscoff, X.; Paukshto, M.V. Some properties of the boundary value problem of linear elasticity in terms of stresses. *J. Elast.* **2004**, *74*, 135–145. https://doi.org/10.1023/B:ELAS.0000033858.20307.d8.
10. Li, S.; Gupta, A.; Markenscoff, X. Conservation laws of linear elasticity in stress formulations. *Proc. R. Soc. A Math. Phys. Eng. Sci.* **2005**, *461*, 99–116. https://doi.org/10.1098/rspa.2004.1347.
11. Kaljevic, I.; Saigal, S.; Hopkins, D.A.; Patnaik, S.N. *Completed Beltrami–Michell Formulation for Analyzing Radially Symmetrical Bodies*; NASA Technical Memorandum 4593; National Aeronautics and Space Administration, Lewis Research Center: Cleveland, OH, USA, 1994; 22p.
12. Georgievskii, D.V. General solutions of weakened equations in terms of stresses in the theory of elasticity. *Mosc. Univ. Mech. Bull.* **2013**, *68*, 1–7. https://doi.org/10.3103/S0027133013010019.
13. Andrianov, I.; Topol, H. Compatibility Conditions: Number of Independent Equations and Boundary Conditions. In *Mechanics and Physics of Structured Media*; Springer: Cham, Switzerland, 2022; pp. 123–140. https://doi.org/10.1016/B978-0-32-390543-5.00011-6.
14. Biffle, J.H.; Becker, E.B. Finite element stress formulation for dynamic elastic-plastic analysis. *Com. Meth. Appl. Mech. Eng.* **1975**, *6*, 101–119. https://doi.org/10.1016/0045-7825(75)90018-3.
15. Bush, L.; Deng, Q.; Ginting, V. A locally conservative stress recovery technique for continuous Galerkin FEM in linear elasticity. *Com. Meth. Appl. Mech. Eng.* **2015**, *286*, 354–372. https://doi.org/10.1016/j.cma.2015.01.002.
16. Olesen, K.; Gervang, B.; Reddy, J.N.; Gerritsma, M. A higher-order equilibrium finite element method. *Inter. J. Num. Meth. Eng.* **2018**, *114*, 1262–1290. https://doi.org/10.1002/nme.5785.

17. Gaur, H. A new stress-based approach for nonlinear finite element analysis. *J. Appl. Com. Mech.* **2019**, *5*, 563–576. https://doi.org/10.22055/JACM.2019.29045.1548.
18. de Almeida, J.P.M.; Reis, J. An efficient methodology for stress-based finite element approximations in two-dimensional elasticity. *Inter. J. Num. Meth. Eng.* **2020**, *121*, 4649–4673. https://doi.org/10.1002/nme.6458.
19. Ambartsumyan, I.; Khattatov, E.; Nordbotten, J.M.; Yotov, I. A multipoint stress mixed finite element method for elasticity on simplicial grids. *SIAM J. Num. Anal.* **2020**, *58*, 630–656. https://doi.org/10.1137/18M1229183.
20. Gaur, H.; Dakssa, L.; Dawood, M.; Samaiya, N.K. A novel stress-based formulation of finite element analysis. *J. Zhejiang Univ.-Sci. A* **2021**, *22*, 481–491. https://doi.org/10.1631/jzus.A2000397.
21. Parrinello, F.; Borino, G. Hybrid equilibrium element with high-order stress fields for accurate elastic dynamic analysis. *Inter. J. Num. Meth. Eng.* **2021**, *122*, 6308–6340. https://doi.org/10.1002/nme.6793.
22. Więckowski, Z.; Świątkiewicz, P. Stress-based FEM in the problem of bending of Euler–Bernoulli and Timoshenko beams resting on elastic foundation. *Materials* **2021**, *14*, 460. https://doi.org/10.3390/ma14020460.
23. Angoshtari, A.; Faghih Shojaei, M.; Yavari, A. Compatible-strain mixed finite element methods for 2D compressible nonlinear elasticity. *Com. Meth. Appl. Mech. Eng.* **2017**, *313*, 596–631. https://doi.org/10.1016/j.cma.2016.09.047.
24. Faghih Shojaei, M.; Yavari, A. Compatible-strain mixed finite element methods for incompressible nonlinear elasticity. *J. Com. Phys.* **2018**, *361*, 247–279. https://doi.org/10.1016/j.jcp.2018.01.053.
25. Yang, Y.; Zhang, S. Mixed finite element methods for elastodynamics problems in the symmetric formulation. *Advan. Appl. Math. Mech.* **2018**, *10*, 1279–1304. https://doi.org/10.4208/aamm.OA-2017-0280.
26. Bertrand, F. Stress-based finite element methods for sea ice dynamics. *Proc. Appl. Math. Mech.* **2018**, *18*, e201800450. https://doi.org/10.1002/pamm.201800450.
27. Viebahn, N.; Schröder, J.; Wriggers, P. An extension of assumed stress finite elements to a general hyperelastic framework. *Adv. Mod. Simul. Eng. Sci.* **2019**, *6*, 9. https://doi.org/10.1186/s40323-019-0133-z.
28. Faghih Shojaei, M.; Yavari, A. Compatible-strain mixed finite element methods for 3D compressible and incompressible nonlinear elasticity. *Comp. Meth. Appl. Mech. Eng.* **2019**, *357*, 112610. https://doi.org/10.1016/j.cma.2019.112610.
29. Meddahi, S.; Ruiz-Baier, R. A mixed discontinuous Galerkin method for a linear viscoelasticity problem with strongly imposed symmetry. *SIAM J. Scien. Com.* **2023**, *45*, 27–56. https://doi.org/10.1137/22M1482081.
30. Meddahi, S. A DG method for a stress formulation of the elasticity eigenproblem with strongly imposed symmetry. *Comp. Math. Appl.* **2023**, *135*, 19–30. https://doi.org/10.1016/j.camwa.2023.01.022.
31. Lamperti, A.; Cremonesi, M.; Perego, U.; Russo, A.; Lovadina, C. A Hu–Washizu variational approach to self-stabilized virtual elements: 2D linear elastostatics. *Com. Mech.* **2023**, *71*, 935–955. https://doi.org/10.1007/s00466-023-02282-2.
32. Sky, A.; Zilian, A. Numerical analysis of the stress-based formulation of linear elasticity. *Proc. Appl. Math. Mech.* **2024**, *24*, e202400185. https://doi.org/10.1002/pamm.202400185.
33. Sky, A.; Zilian, A. Symmetric unisolvent equations for linear elasticity purely in stresses. *Inter. J. Sol. Struc.* **2024**, *295*, 112808. https://doi.org/10.1016/j.ijsolstr.2024.112808.
34. Chen, A.; Sukumar, N. Stress-hybrid virtual element method on quadrilateral meshes for compressible and nearly-incompressible linear elasticity. *Int. J. Num. Meth. Eng.* **2024**, *125*, e7384. https://doi.org/10.1002/nme.7384.
35. Chen, A.; Bishop, J.E.; Sukumar, N. Stress-hybrid virtual element method on six-noded triangular meshes for compressible and nearly-incompressible linear elasticity. *Comp. Meth. Appl. Mech. Eng.* **2024**, *426*, 116971. https://doi.org/10.1016/j.cma.2024.116971.
36. Aguirre, A.; Codina, R.; Baiges, J. Stress–displacement stabilized finite element analysis of thin structures using solid-shell elements, Part I: On the need of interpolating the stresses. *Finite Elem. Anal. Des.* **2024**, *236*, 104168. https://doi.org/10.1016/j.finel.2024.104168.
37. Aguirre, A.; Codina, R.; Baiges, J.; Castañar, I. Stress–displacement stabilized finite element analysis of thin structures using solid-shell elements, Part II: Finite strain hyperelasticity. *Finite Elem. Anal. Des.* **2024**, *236*, 104179. https://doi.org/10.1016/j.finel.2024.104179.
38. Fu, G.; Neunteufel, M.; Schöberl, J.; Zdunek, A. A four-field mixed formulation for incompressible finite elasticity *Comp. Meth. Appl. Mech. Eng.* **2025**, *444*, 118082. https://doi.org/10.1016/j.cma.2025.118082.
39. Kirsch, G. Die Theorie der Elastizität und die Bedürfnisse der Festigkeitslehre. *Z. Des. Vereines Dtsch. Ingenieure* **1898**, *42*, 797–807.
40. Rezini, D.; Khaldi, A.; Rahmani, Y. On the boundary value Kirsch's problem. *J. Mech.* **2016**, *32*, 1–10. https://doi.org/10.1017/jmech.2015.93.

41. Goyat, V.; Verma, S.; Garg, R.K. Reduction in stress concentration around a pair of circular holes with functionally graded material layer. *Acta Mech.* **2018**, *229*, 1045–1060. https://doi.org/10.1007/s00707-017-1974-5.
42. Goyat, V.; Verma, S.; Garg, R.K. Stress concentration reduction using different functionally graded materials layer around the hole in an infinite panel. *Strength Fract. Complex.* **2019**, *12*, 31–45. https://doi.org/10.3233/SFC-190232.
43. Rebora, A.U.; Vernassa, G. Transverse circular holes in cylindrical tubes loaded in traction and in flexion: A new analytical approximation of the stress concentration factor. *Materials* **2020**, *13*, 1331. https://doi.org/10.3390/ma13061331.
44. Liu, X.; Wang, L.; Luo, Q.; Bai, Z.; Li, Q.; Hu, J. A new stress-based formulation for modeling notched fiber-reinforced laminates. *Polymers* **2022**, *14*, 5552. https://doi.org/10.3390/polym14245552.
45. Khaldjigitov, A.; Kalandarov, A.; Djumayozov, U. F. inite-difference equations for 2D elasticity problems on a non-uniform grid. *AIP Conf. Proc.* **2022**, *2637*, 030005. https://doi.org/10.1063/5.0118482.
46. Khaldjigitov, A.; Tilovov, O.; Djumayozov, U. Numerical solution of problem of equilibrium of parallelepiped in stresses. *E3S Web Conf.* **2023**, *401*, 02019. https://doi.org/10.1051/e3sconf/202340102019.
47. Zhukov, M.Y.; Shiryaeva, E.V. *Solving Problems of Mathematical Physics Using the Finite Element Package FreeFem++*; Southern Federal University Publishing House: Rostov-on-Don, Russia, 2014; 256p. (In Russian)